JOURNAL OF SOLID STATE CHEMISTRY 113, 138–144 (1994)

Effects of Divalent Cation Substitution on Sinterability and Electrical Properties of $LaCrO_3$ Ceramics

Fuxue Jin and Tadashi Endo[1]

Department of Molecular Chemistry and Engineering, Faculty of Engineering, Tohoku University, Aramaki, Aoba-ku, Sendai, Miyagi 980, Japan

and

Hirotsugu Takizawa and Masahiko Shimada

Institute for Advanced Materials Processing, Tohoku University, Katahila, Aoba-Ku, Sendai, Miyagi 980, Japan

Received July 12, 1993; in revised form January 25, 1994; accepted January 26, 1994

A series of $LaCr_{1-x}M_xO_3$ (M = Mg, Cu, Zn, Ni) ceramics was fabricated by a conventional sintering process in air and Ar gas. Relative density, electrical conductivity, and magnetic susceptibility were measured to investigate the electrical conduction mechanism of the doped $LaCrO_3$ ceramic. The apparent density was improved up to 95% of theoretical density, especially in the cases of $M = Cu^{2+}$ and Zn^{2+}. The electrical conductivity (σ) increased with increasing quantities of doped divalent cation (x), and $\log(\sigma T)$ showed a linear relationship to ($1/T$). Magnetic data and chemical analysis indicated that the presence of Cr^{4+}, rather than oxygen deficiencies, is preferential for the charge compensation. As a result, the electrical conduction was substantially governed by the hopping of small polarons between Cr^{3+} and Cr^{4+} ions. The substitution of Ni ions resulted in lower than expected unit cell volumes, somewhat different conductivities, and a different antiferromagnetic response, all of which pointed to the role of Ni^{3+} as of the source of an additional band conduction mechanism.

INTRODUCTION

Lanthanum chromite, $LaCrO_3$, has recently received much interest as an electrode material or interconnector for fuel cells, a heating element for high-temperature furnaces, etc. (1–3). However, the electrical conduction mechanism of $LaCrO_3$ ceramics is not well understood. In addition, fully densified $LaCrO_3$ ceramics are frequently required for such applications as those mentioned above. In fact, most practical $LaCrO_3$ ceramics have less than a 75% relative density.

Many investigations have been reported on the sinterability of $LaCrO_3$ ceramics through substitution of Sr^{2+} and Ca^{3+} for La^{3+} (4–7), which indicated that low oxygen activity makes it possible to sinter fully dense $LaCrO_3$ ceramics. Generally, the densification of ceramics is caused by some structure defect, in particular oxygen deficiencies in the lattice. On the other hand, Kose *et al.* (2) demonstrated that the relative electrical conductivity of $La_{1-x}Ca_xCrO_3$ relatively decreased at low oxygen pressure (P_{O_2}), but increased at high P_{O_2}. This was sufficient to show that the oxygen vacancies diminished at high P_{O_2} and the electron holes participated positively in electrical conduction according to the formula $Cr^{4+} = Cr^{3+} + \text{hole}$.

Hayashi *et al.* indicated that both the electrical conductivity and the sinterability of $LaCrO_3$ ceramic could be improved by the substitution of a lower-valence ion such as Cu^{2+}, Mg^{2+}, or Zn^{2+} at the Cr^{3+} site (8). As a result, the formation of oxygen vacancies and Cr^{4+} will be enhanced to preserve electroneutrality with cation stoichiometry, and will influence the electrical properties. As pointed out by Flandermeyer *et al.* (9), Mg^{2+}-substituted $LaCrO_3$ favored either ionic (oxygen vacancy) or electronic (Cr^{4+}) compensation depending on the sintering temperature and oxygen pressure, and the formation of oxygen vacancies scarcely contributed to the improvement of electronic conductivity.

In this paper, sintered $LaCr_{1-x}M_xO_3$ (M = Mg, Cu, Zn and Ni) solid solutions were fabricated and their electrical and magnetic properties were systematically measured to examine the electrical conduction mechanism of the $LaCrO_3$ ceramic.

EXPERIMENTAL

According to the formula $LaCr_{1-x}M_xO_3$, powders of La_2O_3, Cr_2O_3, MgO, CuO, ZnO, and NiO were weighed,

[1] To whom correspondence should be addressed.

0022-4596/94 $6.00

intimately mixed with ethanol for 24 hr, and then dried. The powder mixtures were uniaxally pressed under 100 MPa and then calcined at 900°C for 12 hr in air. After regrinding and reforming, the samples were sintered at temperatures of 1200 to 1600°C for 12 hr in air. Occasionally, the same procedure as described above was carried out in flowing Ar gas in order to examine the electrical characteristics of samples obtained in a different sintering environment.

The phase of products was identified using a Shimadzu XD-610 X-ray powder diffractometer system (Ni-filtered Cu$K\alpha$ radiation). The integrated intensities and the positions of reflections were measured at a scanning rate of 0.25°/min. Silicon powders were used as an internal standard. Accurate unit cell parameters of the product were determined using a least-squares method. The bulk density was measured by Archimedes' technique.

The chemical compositions of the solid solutions were determined by the following procedure. After the sample was dissolved into molten Na_2CO_3 at 1000°C, the mixtures were dissociated in concentrated HNO_3 solution. Cation contents were quantitatively determined by ICP analysis. (Results were La 58.73 wt% and Cr 21.96 wt%. Calculated values for $LaCrO_3$ were La 58.14 wt% and Cr 21.77 wt%.)

The microstructure of the resulting sample was observed by scanning electron microscopy (SEM) using an Akashi Beam Technology ABT-55 scanning microscope.

DC electrical conductivity was measured by means of the standard four-probe technique in the temperature range 300–1073 K in air. Magnetic susceptibility was measured using a Shimadzu MB-11 magnetic torsion balance in the temperature range 78–873 K in He gas.

RESULTS AND DISCUSSION

According to the X-ray powder diffraction patterns, all the solid solutions $LaCr_{1-x}M_xO_3$ (M = Mg, Zn, Cu, and Ni) sintered in air were single phase with orthorhombic perovskite-like structure. Figure 1 shows the unit cell volume as a function of M cation content (x) in $LaCr_{1-x}M_xO_3$. The unit cell volume of $LaCr_{1-x}M_xO_3$ (M = Mg^{2+}, Cu^{2+}, Zn^{2+}) is monotonically increased with increasing x. It was still ambiguous whether the compositional limit of the solid solution was at x = 0.2 or not. However, the present results implied that the lattice Cr^{3+} ions were faithfully replaced in the range x = 0 to 0.2 by divalent cations (Mg, 0.720 Å; Cu, 0.730 Å; Zn, 0.745 Å) with larger ionic radii than Cr^{3+} (=0.615 Å). On the other hand, no appreciable change was observed in the unit cell volume of $LaCr_{1-x}Ni_xO_3$, despite the ionic radius of Ni^{2+} being 0.700 Å. Since the supplementary phases were not observed at $x < 0.2$, it is expected that Cr^{3+} ions were partially or completely replaced by Ni^{3+} ions with ionic radius 0.600 Å (10).

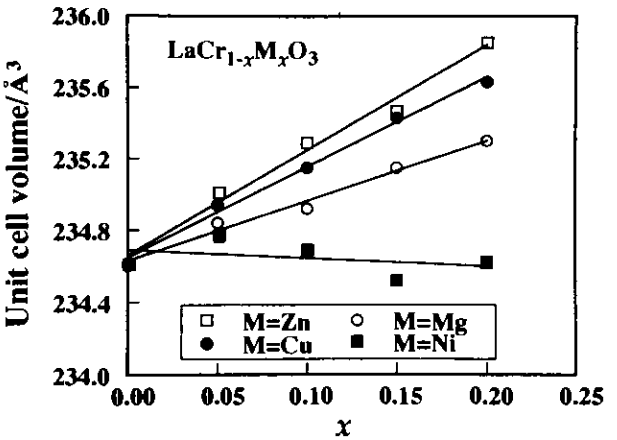

FIG. 1. Unit cell volume of $LaCr_{1-x}M_xO_3$ synthesized for 12 hr in air at 1200°C for M = Cu, 1300°C for M = Ni, 1600°C for M = Mg and Zn.

Figure 2 shows the relative density of the sintered $LaCr_{1-x}M_xO_3$ sample at various temperatures in air. The relative densities of $LaCr_{1-x}M_xO_3$ (M = Mg, Ni) samples are insensitive to the value of x. On the other hand, the densities of $LaCr_{1-x}Cu_xO_3$ samples obviously increased with increasing Cu^{2+} content. In the case of Zn^{2+} substitution, the relative density is practically dependent on the sintering temperature, as seen from the results of sintering samples at 1350°C and 1600°C. The sample sintered at 1600°C has about 95% of the theoretical density. According to the results of the chemical and thermogravimetric analyses, the chemical compositions of the resulting samples corresponded well to the composition of the starting materials within experimental error.

The sinterability of $LaCr_{1-x}M_xO_3$ samples was substantially increased by the formation of the oxygen vacancy, which was accelerated by the thermal diffusion of oxygen. However, the vacancy concentration was related not only

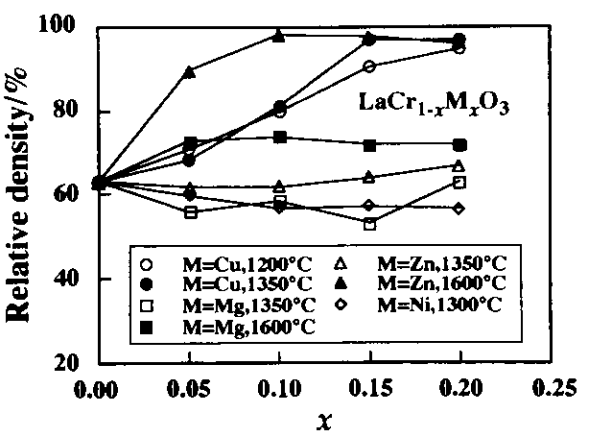

FIG. 2. Relative densities of $LaCr_{1-x}M_xO_3$ (M = Cu, Mg, Zn, Ni) samples sintered at various temperature in air.

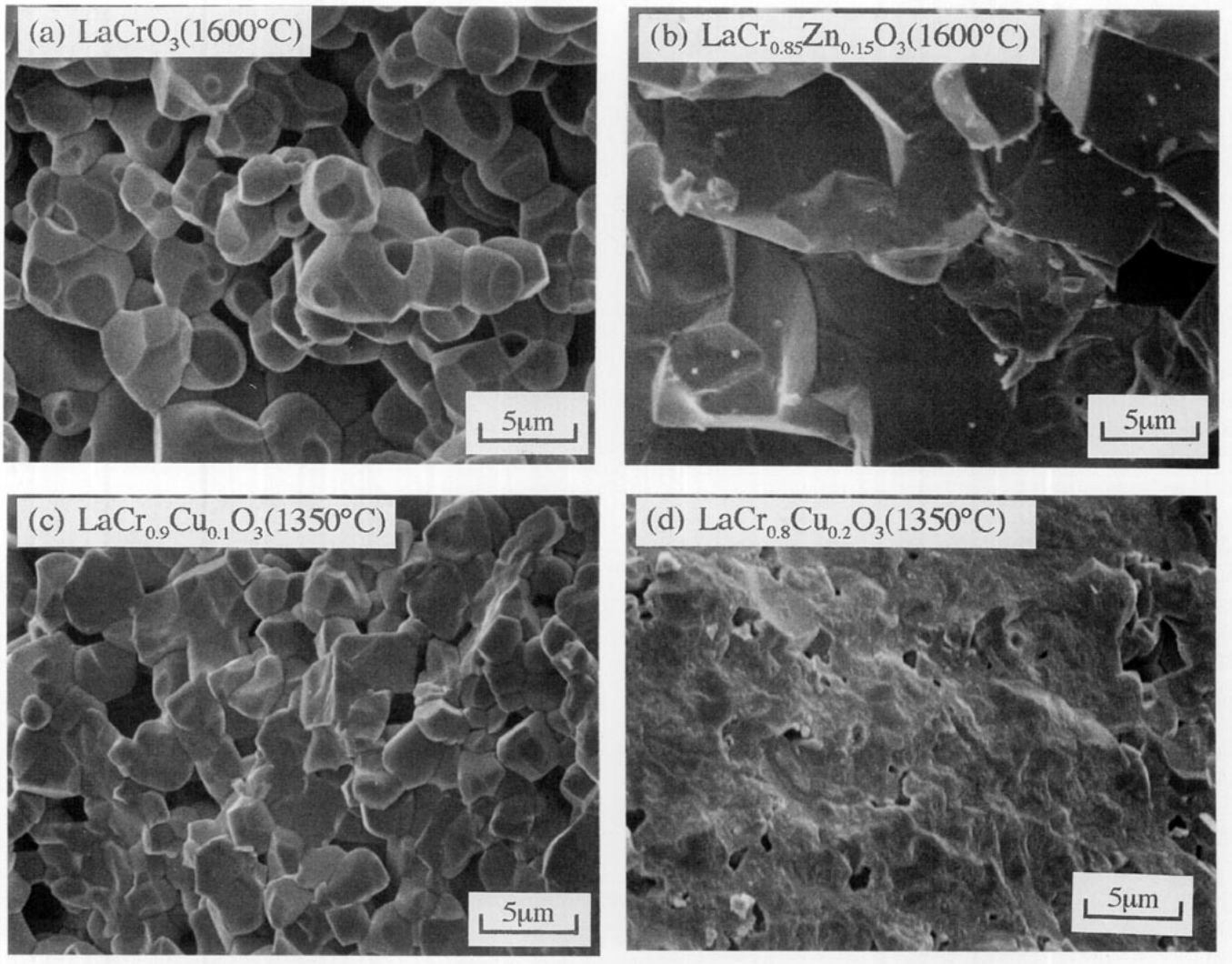

FIG. 3. SEM photographs of the fracture surfaces of (a) $LaCrO_3$ (1600°C), (b) $LaCr_{0.85}Zn_{0.15}O_3$ (1600°C), (c) $LaCr_{0.9}Cu_{0.1}O_3$ (1350°C), and (d) $LaCr_{0.8}Cu_{0.2}O_3$ (1350°C).

to the sintering temperature and oxygen activity, but also to the kind of substituent cations. This complexity has made the sintering process of $LaCrO_3$ difficult to understand.

Figure 3 shows the SEM photographs of the fracture surfaces of (a) $LaCrO_3$ (sintered at 1600°C), (b) $LaCr_{0.85}Zn_{0.15}O_3$ (sintered at 1600°C), (c) $LaCr_{0.9}Cu_{0.1}O_3$, and (d) $LaCr_{0.8}Cu_{0.2}O_3$ (sintered at 1350°C) ceramics, respectively. All the samples described above were sintered in air. The fracture surface of the $LaCrO_3$ ceramic consists of individual grains with irregular shapes as shown in Fig. 3a. In the case of Zn^{2+} substitution, remarkable grain growth is observed as shown in Fig. 3b. The grain size of $LaCr_{0.85}Zn_{0.15}O_3$ is estimated to be about five times as large as that of $LaCrO_3$. The SEM photographs show that the major fracture occurred at the grain boundaries, except for the $LaCr_{0.8}Cu_{0.2}O_3$ ceramic shown in Fig. 3d. In the case of Cu^{2+} substitution, no grain growth is observed in the range of a few micrometers. In addition, the fracture propagates across the intragrains of densified ceramics at high concentrations of Cu^{2+}.

Some samples sintered in Ar gas showed different SEM profiles with large pores, since they were less dense (70–85% relative density) and partially hydrolyzed in humid air. Furthermore, the samples sintered in Ar gas showed dispersive and smaller changes in the unit cell volume than the samples sintered in air with the substitution of M^{2+}. Among them, $LaCr_{0.9}Cu_{0.1}O_3$ and $LaCr_{0.9}Zn_{0.1}O_3$ sintered in Ar gas were regarded as being substantially stable in air.

Figures 4 and 5 show the temperature dependence of the electrical conductivities of $LaCr_{1-x}Cu_xO_3$ and La

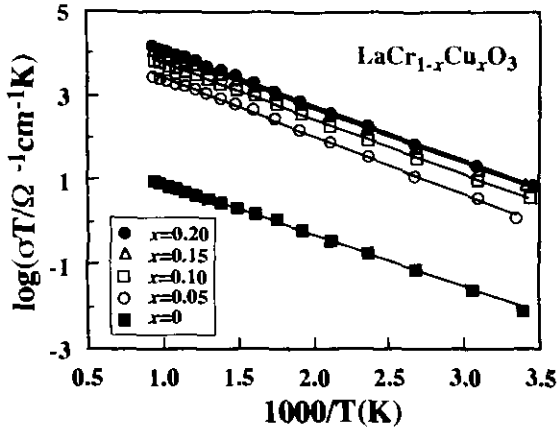

FIG. 4. Temperature dependence of electrical conductivities of La $Cr_{1-x}Cu_xO_3$ sintered at 1200°C for 12 hr in air.

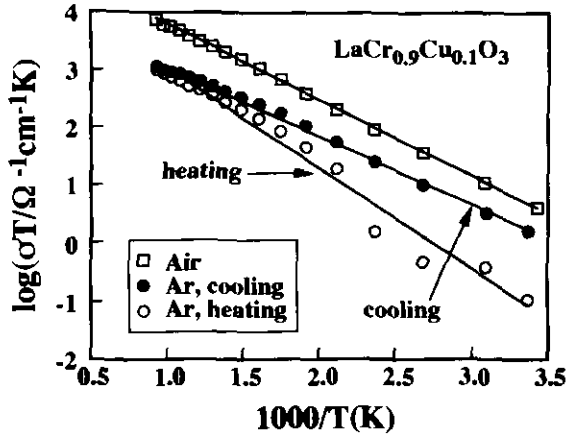

FIG. 6. Temperature dependence of electrical conductivities of $LaCr_{0.9}Cu_{0.1}O_3$ sintered at 1200°C for 12 hr in air and Ar.

$Cr_{1-x}Ni_xO_3$, respectively. The variation of dc conductivities was not fitted by the line between $\log(\sigma)$ and $(1/T)$ which was applicable for a conventional band model. The relationship $\sigma = (C/T)\exp(-E/kT)$, which was generally used for the hopping model was satisfied in the figures, and for the other solid solutions in the studied temperature region. In $LaCr_{1-x}Cu_xO_3$, the slopes of the Arrhenius plot, corresponding to the activation energy (E), are independent of the compositional changes. On the other hand, the slopes of $LaCr_{1-x}Ni_xO_3$ become small as the value of x increases as shown in Fig. 5.

Figures 6 and 7 show the variations of $\log(\sigma T)$ against $(1/T)$ for the $LaCr_{0.9}Cu_{0.1}O_3$ and $LaCr_{0.9}Zn_{0.1}O_3$ ceramics sintered in air and Ar gas, respectively. Note that the measurements of dc conductivity are performed in air. As shown in this figure, the variations of dc conductivity with heating and cooling are essentially due the successive oxidation of samples in air during the measurement of electrical conductivity. Probably some oxygen vacancies of the sample sintered in Ar gas are reduced on heating in air. On cooling, the conductivities of the samples sintered in Ar gas are fairly close to that of the sample sintered in air. Also, the slope of the Arrhenius plot becomes somewhat smaller. Accordingly, the electrical conduction of the samples sintered in air was not intrinsically induced by ionic compensation based on the oxygen vacancy.

The dc conductivity at 300 K and the activation energy (E) of all samples calculated from the slopes of the least-squares fit of $\log(\sigma T)$ against $(1/T)$ are listed in Table 1. The conductivities of $LaCr_{1-x}M_xO_3$ (M = Cu, Mg, Zn) are two to three orders of magnitude higher than that of $LaCrO_3$, and the values of activation energies reduce from 25 to 15 kJ/mol with divalent cation substitution. Bansal *et al.* (11) suggested that the activation energies of La_{1-x}

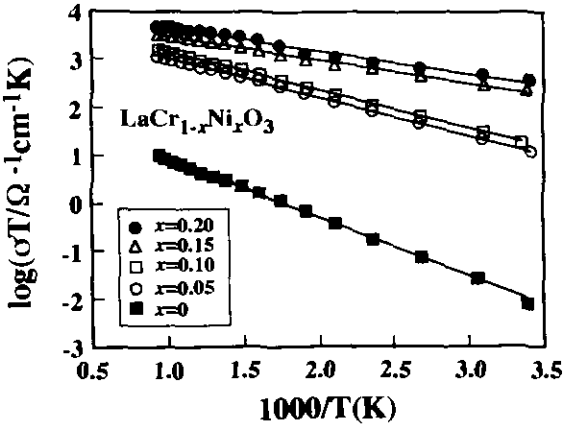

FIG. 5. Temperature dependence of electrical conductivities of La $Cr_{1-x}Ni_xO_3$ sintered at 1300°C for 12 hr in air.

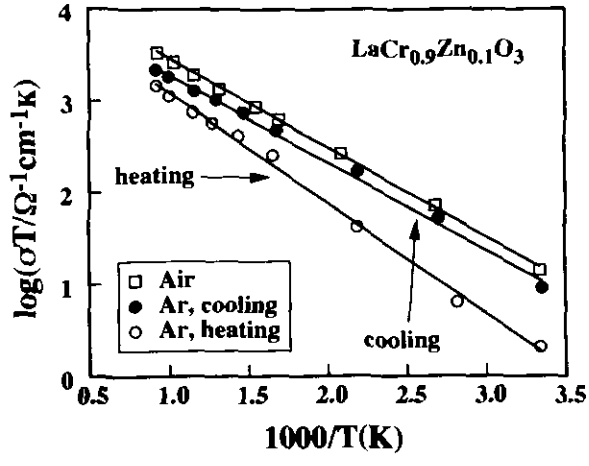

FIG. 7. Temperature dependence of electrical conductivities of $LaCr_{0.9}Zn_{0.1}O_3$ sintered at 1350°C for 12 hr in air and Ar.

TABLE 1
Electrical Conductivity (at 300 K), Activition Energy for $LaCr_{1-x}M_xO_3$

Sample	x	$\sigma(\Omega^{-1}\,cm^{-1})$ at 300 K	E(kJ/mol)
	Sintered in air		
$LaCrO_3$	0	2.1×10^{-5}	24.1
$LaCr_{1-x}Cu_xO_3$	0.1	0.018	25.2
	0.2	0.037	25.1
$LaCr_{1-x}Mg_xO_3$	0.1	0.118	18.1
	0.2	0.132	18.3
$LaCr_{1-x}Zn_xO_3$	0.1	0.167	17.6
	0.2	0.104	15.4
$LaCr_{1-x}Ni_xO_3$	0.1	0.069	10.8
	0.2	1.27	7.4
	Sintered in a stream of Ar		
$LaCr_{1-x}Cu_xO_{3-\delta}$	0.1	3.29×10^{-4}	33.0
	0.2	0.029	19.4

Sr_xCrO_3 were in the range of 13 to 22 kG/mol, and the electrical conduction was controlled by the presence of Cr^{4+} due to Sr^{2+} substitution (12). In this context, the hopping conduction between Cr^{3+} and Cr^{4+} is essentially determined by the number of hopping sites and the activation energy for the mobility of small polarons by the substitution of divalent cation M^{2+} in the solid solution $La Cr_{1-x}M_xO_3$.

Incidentally, the value of the activation energy for $La Cr_{1-x}Ni_xO_3$ is the lowest, and decreases with increasing substituent content (x). Perhaps such a change is not sufficient to account for the conduction mechanism proposed above, but the detailed reason is to be discussed below.

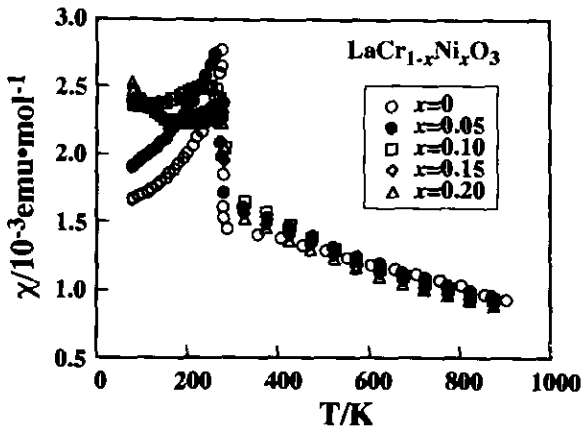

FIG. 9. Magnetic susceptibilities vs temperature for $LaCr_{1-x}Ni_xO_3$ sintered at 1300°C for 12 hr in air.

Figures 8 and 9 show the temperature dependences of the magnetic susceptibilities for $LaCr_{1-x}M_xO_3$ (M = Cu, Ni) sintered in air. Rapid changes of the χ–T slopes are observed in the temperature range from 160 to 270 K. All samples did not prove to be typical antiferromagnetic, as reported by Bansal *et al.* (11) for $La_{1-x}Sr_xCrO_3$. For all samples sintered in air except for $LaCr_{1-x}Ni_xO_3$, the magnetic susceptibility in the paramagnetic region decreased and the Néel temperature became lower with increasing substitution content (x). The increased distance between Cr^{3+} and Cr^{3+}, described as the swelling of the unit cell volume, might participate in the reduction of the Néel temperature.

Figure 10 shows the temperature dependence of magnetic susceptibility for $LaCr_{1-x}Cu_xO_3$ sintered in Ar gas. As seen in this figure, the magnetic susceptibility decreased with increasing Cu^{2+} concentration, but the Néel temperature hardly changed.

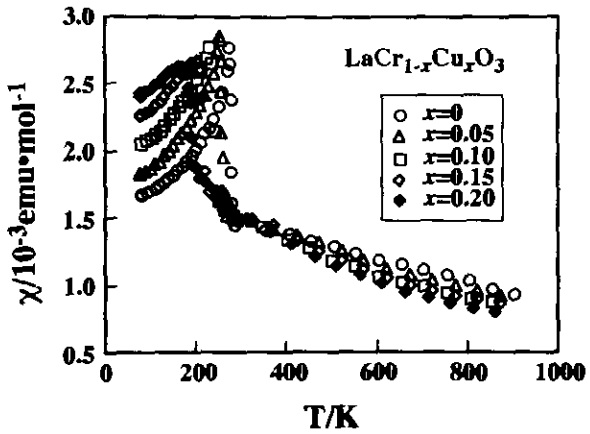

FIG. 8. Magnetic susceptibilities vs temperature for $LaCr_{1-x}Cu_xO_3$ sintered at 1200°C for 12 hr in air.

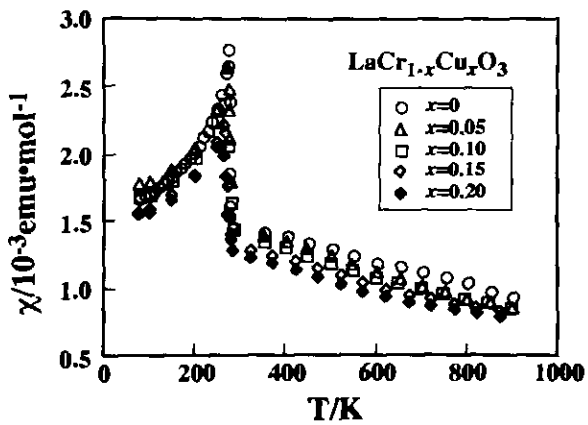

FIG. 10. Magnetic susceptibilities vs temperature for $LaCr_{1-x}Cu_x O_{3-\delta}$ sintered at 1200°C for 12 hr in Ar.

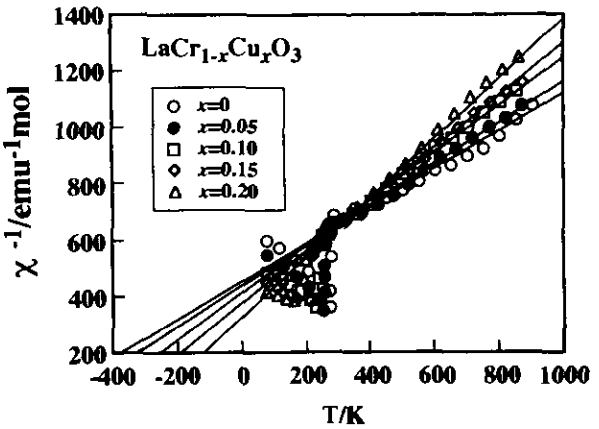

FIG. 11. Reciprocal magnetic susceptibilities vs temperature for La $Cr_{1-x}Cu_xO_3$ sintered at 1200°C for 12 hr in air.

Figures 11 and 12 show the temperature dependences of inverse paramagnetic susceptibilities for $LaCr_{1-x}M_xO_3$ (M = Cu, Ni) samples sintered in air. From the value of the paramagnetic Curie temperature, T_θ, it was estimated that the antiferromagnetic Cr^{3+}–Cr^{3+} interaction was successively weakened by substituting Cu^{2+}, but it was independent of the substitution of Ni ions due to the formation of the trivalent state of the Ni ions.

Table 2 shows the Néel temperatures and the effective magnetic moments of $LaCr_{1-x}M_xO_3$. The spin-only magnetic moment of $LaCr^{3+}O_3$ is calculated to be about $3.873\mu_B$. The observed magnetic moments of the $LaCr_{1-x}M_xO_3$ sintered in air decreased with increasing content of the nonmagnetic divalent cations, i.e., $Mg^{2+}(2p^6)$ and $Zn^{2+}(3d^{10})$. This is due to the decrease in the Cr^{3+} concentration by the substitution of nonmagnetic cations. On the other hand, the magnetic moments of $LaCr_{1-x}Ni_xO_3$ are quite independent of the substitution of Ni ion for Cr^{3+}. The observation was plausible that $Ni^{3+}(3d^7)$, having the same net spins as $Cr^{3+}(3d^3)$, was formed. The observed magnetic moments of $LaCr_{1-x}Cu_xO_3$ sintered in air are somewhat lower than that of $LaCr_{1-x}Cu_xO_3$ sintered in Ar gas. This result indicated that the oxygen vacancies were dominantly formed without the formation of Cr^{4+} in $LaCr_{1-x}Cu_xO_3$ sintered at low-oxygen activity. When the sintering procedure was performed at high oxygen activity, the oxygen vacancies should diminish and the formation of Cr^{4+} should be partially enhanced, as shown in the following relation:

$$LaCr^{3+}_{1-x}Cu^{2+}_x\,O_{3-x/2} \underset{\text{oxidation}}{\overset{\text{reduction}}{\rightleftharpoons}} La(Cr^{2+}_{1-2x}Cr^{4+}_x)Cu^{2+}_x\,O_3.$$

From the shifts of the Néel temperature and the paramagnetic Curie temperature, it was found that the interactions between Cr^{3+} ions were more or less affected by the presence of Cr^{4+}.

TABLE 2

Néel Temperature and Effect Bohr Magneton Number for $LaCr_{1-x}M_xO_3$

Sample	x	Néel temperature	P_{eff}
	Sintered in air		
$LaCrO_3$	0	275	3.63
$LaCr_{1-x}Cu_xO_3$	0.1	230	3.02
	0.2	160	2.71
$LaCr_{1-x}Mg_xO_3$	0.1	225	3.11
	0.2	160	2.76
$LaCr_{1-x}Zn_xO_3$	0.1	240	3.23
	0.2	200	2.91
$LaCr_{1-x}Ni_xO_3$	0.1	250	3.02
	0.2	270	3.01
	Sintered in a stream of Ar		
$LaCr_{1-x}Cu_xO_{3-\delta}$	0.1	267	3.18
	0.2	256	3.07

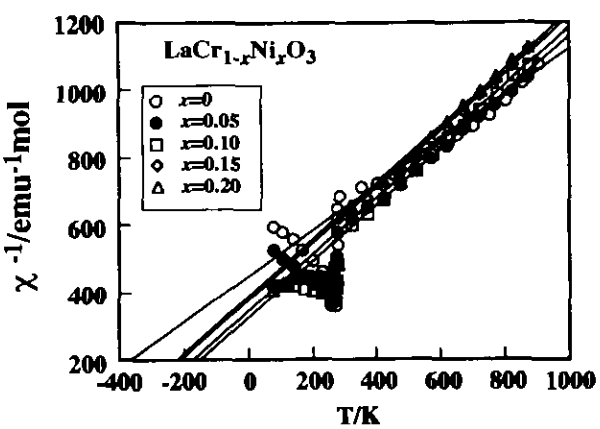

FIG. 12. Reciprocal magnetic susceptibilities vs temperature for La $Cr_{1-x}Ni_xO_3$ sintered at 1300°C for 12 hr in air.

CONCLUSION

The solid solutions with the formula $LaCr_{1-x}M_xO_3$ (M = Cu, Mg, Zn, Ni) were sintered in air. The sinterability of $LaCrO_3$ ceramics was improved by substituting divalent cations such as Cu^{2+} and Zn^{2+} for Cr^{3+}. In addition, the electrical conductivities of the sintering samples were obviously increased by substituting divalent cations (M^{2+}) for Cr^{3+}. Magnetic data showed that the substitution of divalent cations with net spins of <3/2 decreased the

effective Bohr magneton number, and eventually changed the antiferromagnetic contribution of Cr^{3+}–Cr^{3+} couplings. Such observations implied that the electroneutrality of doped $LaCrO_3$ in air was not balanced by oxygen deficiency but by the presence of Cr^{4+}. Consequently, hopping conduction between Cr^{3+} and Cr^{4+} by the mechanism of small polarons was proposed.

In $LaCr_{1-x}Ni_xO_3$ ceramics, the unit cell volume hardly changed with the Ni concentration. Therefore, the substituted Ni ion seemed to be in the trivalent state with close to the ionic radius of Cr^{3+}. The interpretation was also supported by the results that magnetic susceptibilities and Néel temperatures of $LaCr_{1-x}Ni_xO_3$ were almost insensitive to the contents of Ni ion, because Ni^{3+} ($3d^7$) has the same net spins as Cr^{3+} ($3d^3$). In $LaCr_{0.8}Ni_{0.2}O_3$ ceramics, Ni^{3+} fulfilled a significant role as the second electrical carrier which significantly increased the electrical conductivities and lowered the activation energy.

REFERENCES

1. D. B. Meadowcroft, *Br. J. Appl. Phys.* **2,** 1225 (1969).
2. Kose, *Kagakukougyou* **25,** 1384 (1974). [In Japanese]
3. K. Kendall, *Ceram. Bull.* **70**(7), 1159 (1991).
4. L. Groupp and H. U. Anderson, *J. Am. Ceram. Soc.* **59,** 449 (1976).
5. N. Sakai, T. Kawada, H. Yokokawa, and M. Dokiya, *J. Mater. Sci.* **25,** 4531 (1990).
6. K. Matsumoto and T. Sata, *Yogyo-Kyokaishi* **89,** 68 (1981). [In Japanese]
7. K. Matsumoto and T. Sata, *Yogyo-Kyokaishi* **89,** 124 (1981). [In Japanese]
8. S. Hayashi, K. Fukaya, and H. Saito, *J. Mater. Sci. Lett.* **7,** 457 (1988).
9. B. K. Flandermeyer, M. M. Nasrallah, A. K. Agarwal, and H. U. Anderson, *J. Am. Ceram. Soc.* **67,** 195 (1984).
10. R. D. Shannon and C. T. Prewitt, *Acta Crystallogr. Sect. B* **25,** 925 (1969).
11. K. P. Bansal, S. Kumari, B. K. Das, and G. C. Jain, *J. Mater. Sci.* **18,** 2095 (1983).
12. D. P. Karim and A. T. Aldred, *Phys. Rev. B* **20**(6), 2255 (1979).